

# Ultrafast Excited-State Deprotonation and Electron Transfer in Hydroxyquinoline Derivatives

Taeg Gyum Kim and Michael R. Topp\*

Department of Chemistry, University of Pennsylvania, Philadelphia, Pennsylvania 19104

Received: June 29, 2004; In Final Form: September 8, 2004

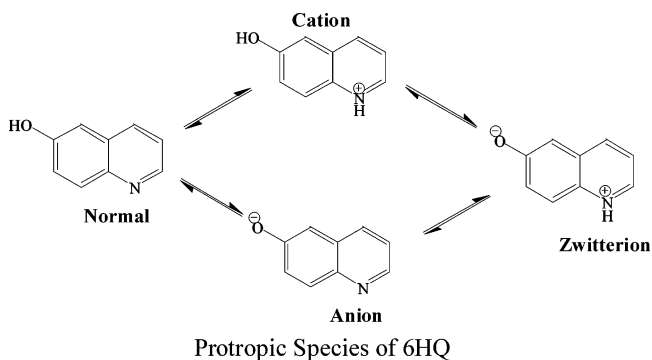
Excited-state proton transfer, electron transfer, and solvent relaxation processes in *N*-methyl-6-hydroxyquinolinium (NM6HQ<sup>+</sup>) and *N*-methyl-7-hydroxyquinolinium (NM7HQ<sup>+</sup>) iodides have been investigated in both acidic and basic solutions. The hydroxyl group behaves like a superacid in the excited state, exhibiting deprotonation times in acidic aqueous solution for NM6HQ<sup>+</sup> and NM7HQ<sup>+</sup> of 2.0 and 4.5 ps, respectively. These rates for intermolecular proton transfer to water molecules are among the fastest reported to date. This high photoacidity correlates with ultrafast intramolecular electron transfer from the hydroxylate (–O<sup>–</sup>) group to the positively charged pyridinium ring, which can be observed in separate measurements in basic solution, where the ground states exist as the deprotonated neutral forms *N*-methyl-6-oxyquinolinium (NM6OQ) and *N*-methyl-7-oxyquinolinium (NM7OQ). The most obvious effect in basic solution is a Stokes shift resulting from solvent relaxation (1.0 ps), driven by the dipole moment change resulting from ultrafast excited-state electron transfer, apparently on the time scale <450 fs. Studies of such coupling between proton transfer and electron transfer offer to provide new insights into the interpretation of other phototautomerization processes.

## I. Introduction

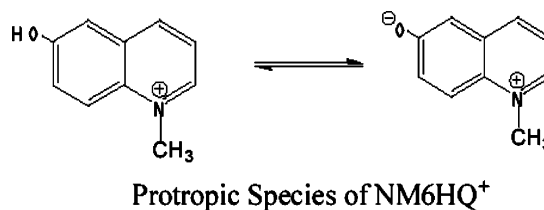
Proton transfer and electron transfer reactions have attracted much attention as topics of central importance in a variety of chemical and biological processes.<sup>1–4</sup> The acidity of hydroxyaromatic compounds tends to increase upon electronic excitation,<sup>5–11</sup> making such compounds useful substrates for examining fundamental aspects of proton transfer using time-resolved fluorescence measurements. Most such compounds studied have shown upon excitation a reduction in p*K*<sub>a</sub> of 6–8 units. This greatly shifts the acid–base equilibrium, causing excited-state proton transfer to an aqueous solvent on a nanosecond time scale, although the proton transfer times to other solvents may be longer than the excited-state lifetime. For example, in the case of 2-naphthol, the proton transfer time constant in aqueous solution is ~5 ns, which is comparable to the 10 ns fluorescence decay time.<sup>12</sup> The molecules 6- (6HQ) and 7-hydroxyquinoline (7HQ) exhibit more extreme behavior, because the hydroxyl groups in aqueous solution undergo reductions in p*K*<sub>a</sub> of ~9–11 units.<sup>11</sup> For such cases, proton transfer rates are expected to be much faster, so that excited-state acid–base equilibria can be explored in a wider range of solvents.

The photoinduced tautomerization of 7-hydroxyquinoline and its derivatives has been studied by a number of groups. The solvent-bridge proton relay mechanisms in methanol and water solutions have been of particular interest, as these illustrate a potentially important solvent-mediated pathway for phototautomerization.<sup>5,13–17</sup> This effect has been studied in both the excited and ground states.<sup>6</sup> Bardez et al.<sup>18</sup> reported measurements on the 5-, 6-, 7- and 8-hydroxyquinolinium ions and their derivatives used as polarity- or pH-sensitive probes. Recently, Jang and co-workers<sup>11</sup> used streak camera techniques at ~10 ps resolution to examine the tautomerization of excited 6-HQ, focusing on the likely catalytic roles of H<sub>3</sub>O<sup>+</sup>, OH<sup>–</sup>, and H<sub>2</sub>O

as a function of pH in the internal proton transfer process. However, the mechanism of tautomerization between the zwitterion and keto species in hydroxyquinoline molecules is still not well understood.



For 6HQ and 7HQ, the two prototropic functional groups yield four prototropic species including a “normal” molecule, an OH-deprotonated anion, an N-protonated cation, and an OH-deprotonated, N-protonated zwitterion, all in equilibrium in aqueous solution.<sup>6,11,19</sup> On the other hand, blocking the nitrogen atom to protonation by methyl substitution can simplify the problem. Thus the *N*-methyl cationic derivatives of 6HQ and 7HQ, which are termed *N*-methyl-6-hydroxyquinolinium (NM6HQ<sup>+</sup>) and *N*-methyl-7-hydroxyquinolinium (NM7HQ<sup>+</sup>),



reveal only two prototropic species, a cation (low pH) and a

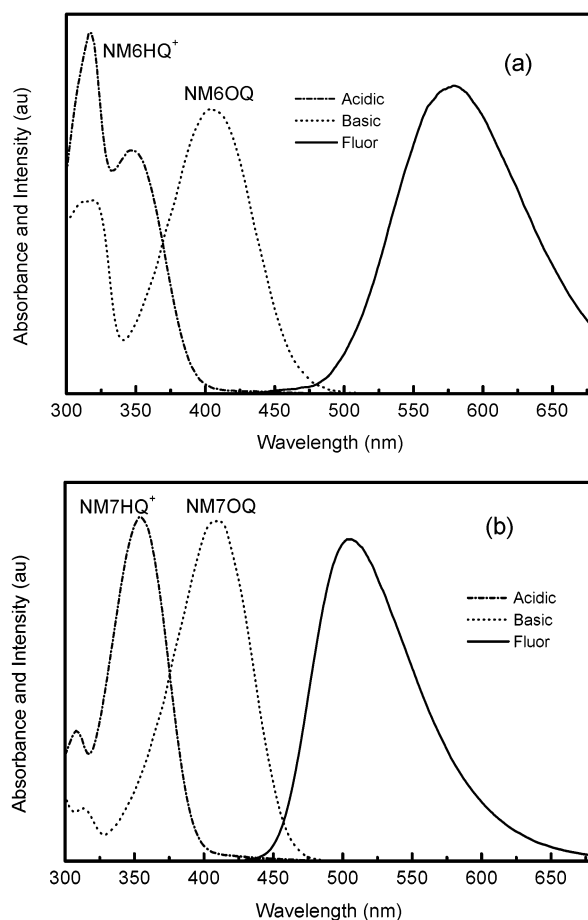
\* To whom correspondence should be addressed. Telephone: Tel: 1-215-898-4859. Fax: 1-215-573-2112. E-mail: mrt@sas.upenn.edu.

zwitterion (high pH) in aqueous solution.<sup>18,20</sup> It is likely that the zwitterions in hydroxyquinoline molecular systems may undergo intramolecular electron transfer from the deprotonated  $-O^-$  group to the aromatic ring to produce a keto tautomer. Aqueous solutions of  $NM6HQ^+$  and  $NM7HQ^+$  are potentially more convenient than  $6HQ$  and  $7HQ$  to survey excited-state intramolecular electron transfer phenomena on an ultrashort time scale, because the ground states of these molecules exist in weakly basic solution as zwitterions. Finally, it has been shown that the  $NM6HQ^+$  cation exhibits such a strong photoacidity that photoinduced deprotonation of the hydroxyl group can occur even in 10 M perchloric acid solution.<sup>18</sup> This strong photoacidity is likely to result from intramolecular electron transfer coupled to the deprotonation of the  $-OH$  group, where the presence of the electron-withdrawing moiety ( $\geq N^+-CH_3$ ) actually amplifies the photoacidity of the  $-OH$  group.

In weakly acidic solution (pH  $\sim 3$ ), the absorption spectra of  $6HQ$  and the *N*-methyl cation,  $NM6HQ^+$ , in the 300–500 nm region are almost the same. In both cases, the oxygen atom is protonated, and the presence of the methyl group on the nitrogen atom evidently has little effect on the absorption spectrum in this region. The (time-integrated) emission spectra in acidic solution are also the same, because in both cases the emitting species contains the deprotonated oxygen atom, and emission is likely to come from the keto form.<sup>18</sup> On the other hand, the two molecules behave differently in basic solution, because the absorbing species for  $6HQ$  is the anion,  $6OQ^-$ , which has a maximum at 360 nm, whereas for  $NM6HQ^+$ , the absorber is the zwitterion,  $NM6OQ$ , which has a maximum at 410 nm (see Figure 1). In both acidic and basic solutions, the primary emitting species for both substances is the same (i.e., the keto form), but for the species  $6HQ$  in basic solution, there is also intermediate emission from the anion, before the nitrogen atom becomes protonated by the solvent. Finally, at pH 7, the absorption and emission spectra of the parent molecules contain another component. For example, for  $6HQ$ , the dominant absorbing species is a “normal” molecule, and there are three components in the emission spectrum, including the “normal” molecule, the anion and the keto tautomer.<sup>11</sup> However, for the *N*-methyl derivative,  $NM6HQ^+$ , only the keto form contributes significantly to the emission spectrum, which is evidence that the deprotonation of the  $-OH$  group occurs on a much shorter time scale.

The ground-state prototropic equilibria are governed by the  $pK_a$  values, which, for the  $-OH$  groups of  $NM6HQ^+$  and  $NM7HQ^+$ , are about 7.0 and 6.0, respectively.<sup>20,21</sup> Thus, both compounds exist almost exclusively in the protonated form at pH 3 (0.001 M HCl) and in the deprotonated form at pH 11 (0.001 M NaOH). Under weakly acidic conditions, the absorption spectra of both  $NM6HQ^+$  and  $NM7HQ^+$  show maxima around 355 nm, whereas in basic solution, the band lies near 410 nm. The time-integrated emission spectrum of each species is the same at pH 3 and pH 11, the maxima falling at 580 nm ( $NM6HQ^+$ ) and 510 nm ( $NM7HQ^+$ ) (see Figure 1). The time-integrated emissions originate mostly from the deprotonated form ( $Z^*$  and  $K^*$ ) because the proton transfer rates from  $-OH$  to water are too fast to observe emission from the originally populated state ( $C^*$ ) under weakly acidic conditions.

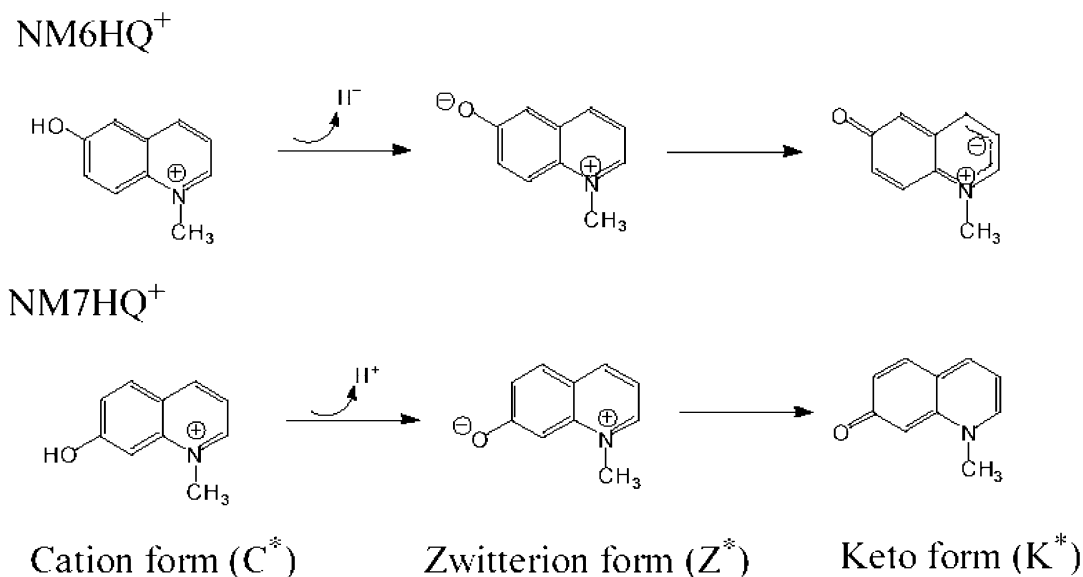
Excited-state proton and electron transfer phenomena in molecules possessing proton donor and acceptor groups are usually described in terms of electronic coupling between the locally excited state reached by Franck–Condon excitation of the ground state (here, the zwitterion form) and the charge transferred state (keto form). The driving force of the photo-



**Figure 1.** Absorption and emission spectra of *N*-methyl-6-hydroxyquinolinium iodide ( $NM6HQ^+ I^-$ ) (a) and *N*-methyl 7-hydroxyquinolinium iodide ( $NM7HQ^+ I^-$ ) (b) in acidic (0.001 M HCl) and basic (0.001 M NaOH) aqueous solutions. The cations are deprotonated in basic solution and are relabeled  $NM6OQ$  and  $NM7OQ$ , respectively. The absorption spectra have longest wavelength absorption maxima at 350 and 355 nm in acidic conditions and at 405 and 410 nm in basic conditions, respectively. However, their emission spectra in acid condition exactly coincide with those in basic condition showing respective emission maxima at 580 and 510 nm.

induced processes comes from the large changes of the acidity and basicity of the groups involved. In hydroxyquinolines, this process will lead to a large decrease of the dipole moment, and consequently to a marked solvatochromic effect. It is still a point of discussion as to whether a hydroxyquinoline molecule in the ground and excited states has a zwitterion form with large charge separation or a keto form with reduced charge separation. The excited keto form ( $K^*$ ) is obtained if intramolecular electron transfer occurs from the  $-O^-$  group of the excited zwitterion form ( $Z^*$ ) to the neighboring ring. However, before the present work, no evidence had been published that could distinguish the  $Z^*$  and  $K^*$  forms. Bardez et al.<sup>18</sup> studied the solvatochromism of  $NM6HQ^+$  in 1,4-dioxane and water (pH 10) mixtures, where they attributed the structure of aqueous *N*-methyl-6-oxyquinolinium in the ground state to the  $Z^*$  form. They argued that, in the ground state, a less polar solvent would tend to favor a resonance hybrid structure shifted in the direction of the less polar resonance forms. In the excited state, the deprotonated forms of the two molecules can exist as the charge separated  $Z^*$  and charge recombined  $K^*$  forms, as shown in Scheme 1.

In this article, we report spectroscopic data obtained by ultrafast techniques that illustrate the strong photoacidity of these

SCHEME 1 : Excited-State Species of *N*-Methyl-6-hydroxyquinolinium and *N*-Methyl-7-hydroxyquinolinium

molecules and the relaxation events that follow electronic excitation of the *N*-methyl-6- and 7-hydroxyquinolinium ions for both acidic and basic solutions. The similarity in behavior of 6- and 7-hydroxyquinolinium species will also be confirmed. Moreover, the results presented here allow us to show clear evidence of adiabatic electron transfer from Z\* to K\*.

## II. Experimental Section

*N*-Methyl-6- and 7-hydroxyquinolinium iodides were prepared by refluxing 6- and 7-hydroxyquinoline with methyl iodide in dry toluene for 48 h. The solid product was precipitated by adding ether and recrystallized twice in an ethanol–ether mixture. The experimental samples were prepared by dissolving *N*-methyl-6- and 7-hydroxyquinolinium iodides in water containing either 0.001 M NaOH or 0.001 M HCl.

For measurements of the fluorescence lifetime, an ultrafast fluorescence upconversion setup was used. The apparatus was based on a self-mode-locked titanium sapphire oscillator,

including a double-prism compressor, pumped by second-harmonic radiation from a Nd:YVO<sub>4</sub> laser (Coherent Verdi). The output at ~100 MHz was fed through a multipass amplifier (Quantronix Odin), including a stretcher/compressor pair, which was pumped by the second harmonic of a Q-switched Nd:YLF laser (Quantronix 527). The experiments, for which a schematic diagram is shown in Figure 2, employed fundamental pulses at ~1 kHz repetition rate from the amplified Ti:sapphire laser, delivering 200 mW near 800 nm. Second-harmonic radiation near 400 nm, generated by type-I phase-matching in a 0.1 mm BBO crystal, was used for excitation. Because of differences in the absorption spectra, the laser oscillator was tuned so that the second harmonic spectrum was centered at 397 and 410 nm for acidic and basic solutions, respectively (see Figure 1). The polarization of the excitation pulses was controlled by a half-wave plate before focusing into a flowing sample cell with a sample thickness of 1 mm. The temperature was 22 °C. The forward-emitted fluorescence was collected and focused into a

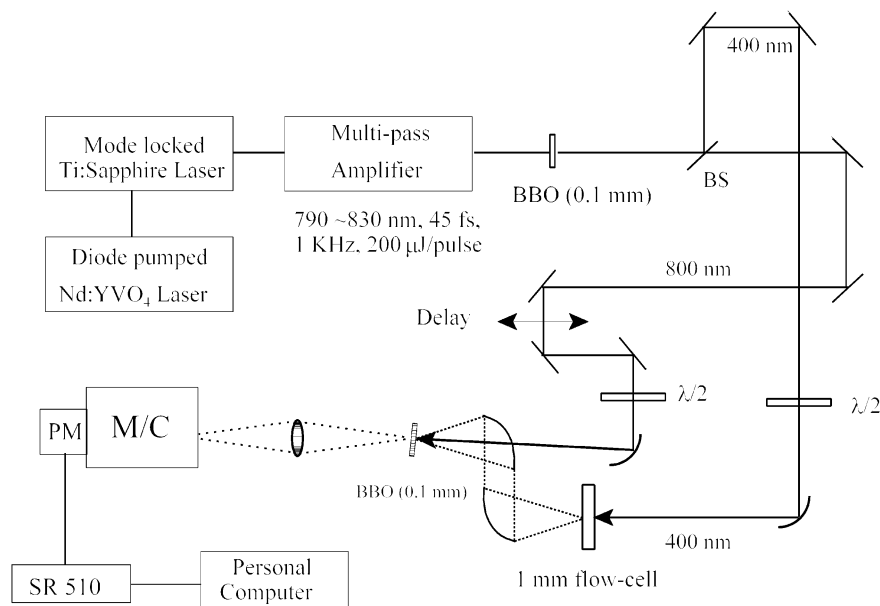


**Figure 2.** Schematic view of the experimental setup for the femtosecond fluorescence upconversion spectrometer: BS, dichroic beam splitter; MC, monochromator; PM, photomultiplier; SR510, signal averager.

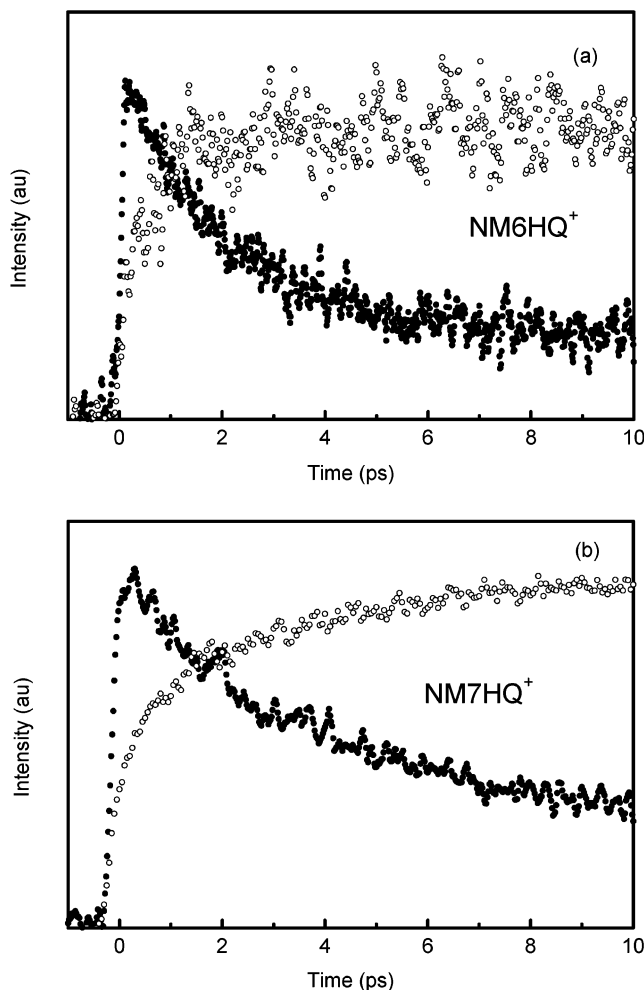


**Figure 3.** Kinetic profiles of *N*-methyl-6-hydroxyquinolinium (NM6HQ<sup>+</sup>) (a) and *N*-methyl-7-hydroxyquinolinium (NM7HQ<sup>+</sup>) (b) in acidic aqueous solution, upon excitation near 397 nm. The monitored wavelengths in NM6HQ<sup>+</sup> solution were 480 nm (solid circles) and 580 nm (open circles) and those in NM7HQ<sup>+</sup> solution were 450 nm (solid circles) and 510 nm (open circles). The spectra in acid solution were significantly weaker than those in basic solution, because of poorer spectral overlap between the laser power spectrum and the sample absorption spectrum.

0.1 mm BBO crystal by a pair of elliptical reflectors. The residual fundamental beam was passed through a variable delay and focused into the BBO crystal by a 30 cm focal length gold mirror to serve as the gate pulse for up-converting the sample fluorescence. The up-converted radiation produced by Type-I phase matching in the BBO crystal was passed through a color filter and detected by a photomultiplier tube mounted on a double monochromator. The output was fed to a lock-in amplifier and to a computer. The overall instrumental response of this system (fwhm) was typically  $\sim 150$  fs, as measured from the solvent Raman signal, measured near 470 nm.

### III. Results and Discussion

**Acidic Solution.** As noted above, both NM6HQ<sup>+</sup> and NM7HQ<sup>+</sup> are protonated at the oxygen atom at pH 3. Recall that the absorption maxima for the two cations are at the same wavelength of 355 nm. Figure 3 shows examples of the decay kinetics of both species in acidic solution, monitored at 450 and 480 nm, for which the lifetimes of NM6HQ<sup>+</sup> and NM7HQ<sup>+</sup> are 2.0 and 4.5 ps, respectively. The analysis of these traces is summarized in Table 1. On the other hand, the emission spectra

**TABLE 1: Fluorescence Time Constants<sup>a</sup>**

samples	monitored wavelengths (nm)	decay time (ps)
NM6HQ <sup>+</sup> in acidic solution	480	2.0 $\pm$ 0.1
NM7HQ <sup>+</sup> in acidic solution	450	4.5 $\pm$ 0.2
NM6OQ in basic solution	500	0.45 $\pm$ 0.05
NM7OQ in acidic solution	470	0.49 $\pm$ 0.05

of the two species have markedly different wavelength maxima. Time profiles, measured at 580 and 510 nm, respectively, for NM6HQ<sup>+</sup> and NM7HQ<sup>+</sup>, reflect the growth of the product state for the two species. Considering that the emission spectra are independent of pH, we interpret the decay kinetics to imply rapid deprotonation of the cations. These rates are among the fastest reported to date for intermolecular proton transfer to an aqueous solvent, and may be attributed to superacidity of the  $-OH$  group in the excited state. For reference, these values are approaching the time scale of, but are probably not yet limited by, the Debye relaxation time of water, which is  $\sim 1$  ps.<sup>22–25</sup> We note also that the excited-state proton dissociation rate of NM6HQ<sup>+</sup> is about twice as fast as that of NM7HQ<sup>+</sup>.

**Basic Solution.** Removal of the hydroxyl proton in basic solution generates the neutral species, which we designate *N*-methyl-6-oxyquinolinium (NM6OQ) and *N*-methyl-7-oxyquinolinium (NM7OQ). This is expected to be in the zwitterionic form (Z). Faster dynamics are revealed when the deprotonated ground states are excited in basic solution; now, the deprotonation step is no longer rate limiting. Thus, Figure 4 shows time profiles for NM6OQ (a) and NM7OQ (b) following excitation of the Z forms in basic solution. Now, comparison between the time profiles recorded at the maxima of the zero-time and longer-term emission spectra do not show a simple complementary behavior, as was seen in Figure 3. Instead, analysis shows that there is a rapid Stokes shift of the emission spectrum on the time scale of  $\sim 1$  ps, with indications of an even faster component on the short-wavelength edge. Such a Stokes shift suggests that there is a substantial change in solvent–solute interactions between the ground and excited states, indicating that there is a large change in the dipole moment.

Bardez et al.<sup>18</sup> reported that the static absorption spectrum of NM6OQ showed negative solvatochromic shifts. That is, the  $\lambda_{\text{max}}$  value increased from 408 nm in pure water to 466 nm in a 1,4-dioxane/water mixture containing 5.3% water. They asserted that the electronic transition from the ground to the excited state involves instantaneous intramolecular charge transfer, leading to an electron distribution in the excited state that is much less dipolar than in the ground state. However, other studies of the excited 6-hydroxyquinolinium ion (or 5-, 7-, 8-hydroxyquinolinium variants) have argued<sup>6,20,26–28</sup> that the deprotonation of the hydroxyl group leads to a Z\* form with an oxy  $-O^-$  group and a quinolinium  $NH^+$  moiety. None of the earlier work showed kinetic evidence of the distinction between Z\* and K\*, which correspond to significantly different  $\pi$ -electron distributions. The kinetic data shown here for *N*-methyl-6-oxyquinolinium and *N*-methyl-7-oxyquinolinium cations may provide evidence for both Z\* and K\* forms in the excited state. The data shown in Figures 4 and 5 clearly indicate the occurrence of an ultrafast electronic relaxation on a faster time scale than the deprotonation step in acid solution. We suggest that spectra show evidence for a rapid intramolecular charge transfer from the  $-O^-$  group to the positively charged pyridinium ring, which also occurs following proton dissociation of the acid form.

To interpret the spectral time evolution more clearly, time profiles similar to Figure 4 were obtained for detection



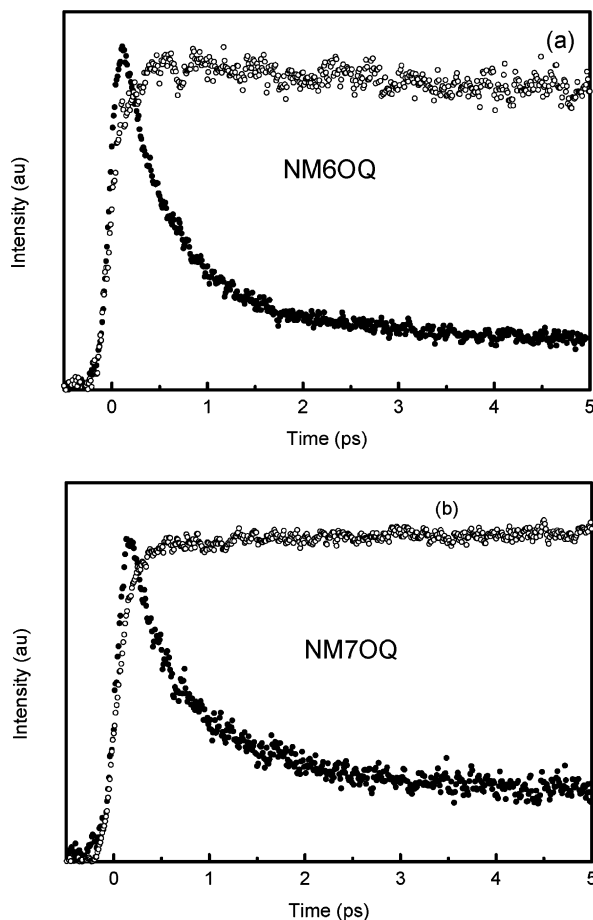


**Figure 4.** Kinetic profiles of *N*-methyl-6-oxyquinolinium (NM6OQ) (a) and *N*-methyl 7-oxyquinolinium (NM7OQ) (b) in basic aqueous solution, upon excitation near 405 nm. The monitored wavelengths in 6OQM solution were 500 nm (solid circles) and 580 nm (open circles) and those in 7OQM solution were 470 nm (solid circles) and 510 nm (open circles).

wavelengths at approximately 5 nm intervals, spanning the range 450–600 nm for NM7OQ solution and 475–640 nm for the NM6OQ case. From these time profiles were compiled time-evolving emission spectra, some of which are shown in Figure 5. Quite clearly, for the NM6OQ case, the spectrum recorded simultaneously with the excitation pulse exhibits a maximum near 520 nm, which is more than 50 nm to shorter wavelengths than the spectrum measured after even 5 ps. We note that the latter is similar to the time-integrated spectrum shown in Figure 1. The NM7OQ case shows a similar but smaller shift (i.e., 470 to 510 nm) on a similar time scale. These spectra monitored at different times after excitation upon excitation of the deprotonated forms (NM7OQ and NM6OQ) may show evidence for two distinct  $Z^*$  and  $K^*$  forms (Figure 5b,c). The time-dependent fluorescence shift provides a direct measurement of the kinetics of solvation occurring at a microscopic level in the aqueous solution. Thus, upon electronic excitation at 410 nm, the fluorescence spectra are progressively shifted to longer wavelengths as the aqueous solvent reequilibrates to the new excited-state charge distribution. In analyzing the time dependence of the spectra, it is useful to work with the normalized spectral shift correlation function  $C(t)$  defined by Maroncelli and Fleming<sup>29</sup> as

$$C(t) = \frac{\nu(t) - \nu(\infty)}{\nu(0) - \nu(\infty)}$$

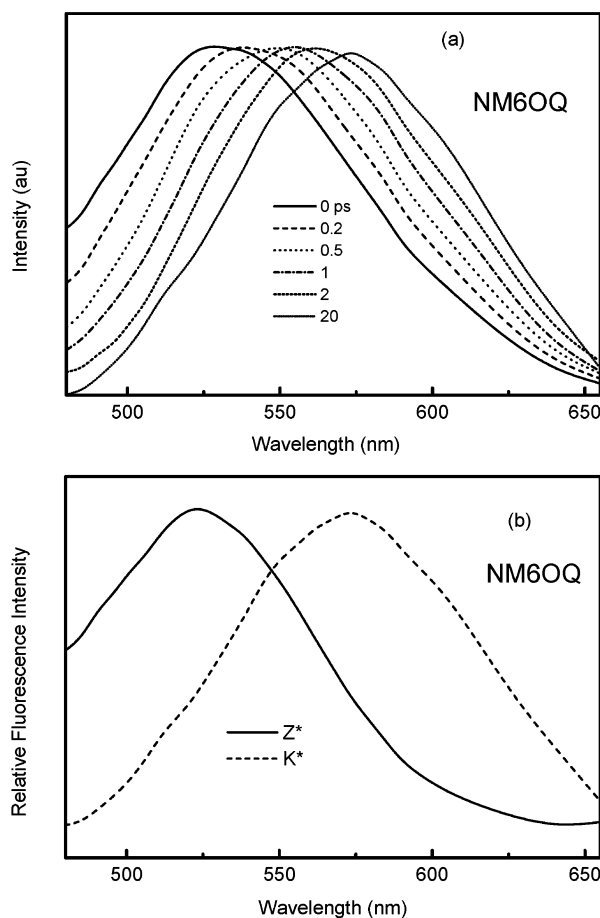


**Figure 5.** Time-resolved spectra of NM6OQ (a) in basic aqueous solution at different delay times, following excitation at 405 nm. The lines represent a smooth curve through 26 experimental data points in each case. Difference spectra showing the zero-time and longer-time forms of NM6OQ (b) and NM7OQ (c), were obtained by comparing kinetic spectra at 20 ps delay with those at zero delay, and with the time-integrated emission spectra, shown in Figure 1.

where  $\nu(t)$ ,  $\nu(0)$ , and  $\nu(\infty)$  are the frequencies of the fluorescence maxima at times  $t$ , 0, and  $\infty$ . For the record, each of the gated fluorescence spectra recorded synchronously with the excitation pulse showed a clear solvent Raman signal peaking near 470 nm. This signal, which was of magnitude similar to that of the gated emission, was readily subtracted from the spectra before compilation of those shown here. No other evidence of artifact was found in the spectra.

The spectral shift correlation function  $C(t)$  of NM6OQ shows almost the same time dependence as that of NM7OQ, as can be seen in Figure 6. The  $C(t)$  kinetics appear to show two decay components having lifetimes of  $\sim 220$  fs and  $\sim 1.04$  ps (see Figure 5 caption). We suggest that the faster component, which is not readily separated from the instrument response function, may reflect electron transfer from  $-O^-$  to the aromatic ring system, leading from the  $Z^*$  form to  $K^*$  whereas the slower one is due to a Stokes shift caused by solute–solvent relaxation.

In summary, it is important to distinguish between the two types of kinetics shown in acidic and basic solutions. The complementary traces in Figure 3 indicate that the process in acid solution is of the kind AB, where the spectrum of A is replaced by that of B. That is, this is a relatively slow process evidently limited by proton transfer. On the other hand, the data of Figures 5 and 6 show that the dynamics appear to be different at different points in the spectrum, revealing a Stokes shift of the emission spectrum. This is why it is necessary to follow

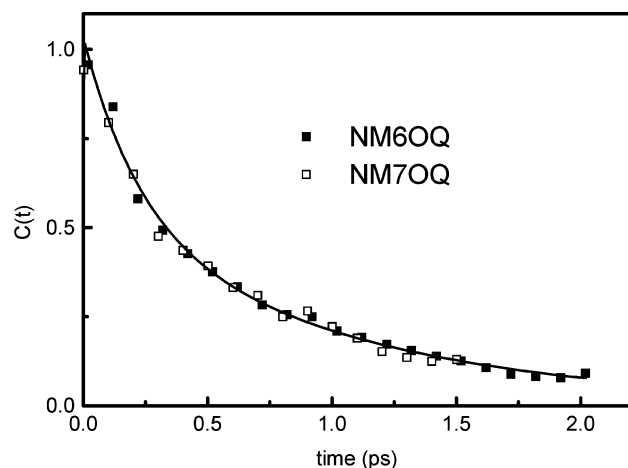


**Figure 6.** Normalized spectral correlation function,  $C(t)$  of NM6OQ (filled squares) and NM7OQ (open squares) in basic solution, upon excitation at 405 nm. The fitted curve had the following parameters:  $I(t) = 0.50 \exp(-t/0.22) + 0.53 \exp(-t/1.04)$ , where the times are in units of picoseconds. Limiting frequency values used in computing  $C(t)$ : 6OQM,  $\nu_0 = 19\,200 \text{ cm}^{-1}$ ,  $\nu_\infty = 17\,200 \text{ cm}^{-1}$ ; 7OQM,  $\nu_0 = 20\,200 \text{ cm}^{-1}$ ,  $\nu_\infty = 19\,600 \text{ cm}^{-1}$ . The spectra, as shown in Figure 5, involved 26 different wavelengths over the range 480–655 nm (6OQM) and 450–600 nm (7OQM), respectively.

the process through the correlation function indicated above. The observed shift on the time scale near 1 ps reflects solvation relaxation dynamics.

Finally, we note that the last observation of a 1 ps relaxation time constant in aqueous solution compares quite well with reported results from some theoretical and experimental determinations made elsewhere. Thus, water relaxation around a dissolved solute molecule has been studied by using the molecular dynamics method. Engström et al.<sup>30</sup> used molecular dynamics computer simulations to study quadrupole relaxation mechanisms for  $\text{Li}^+$ ,  $\text{Na}^+$ , and  $\text{Cl}^-$  ions in dilute aqueous solution. Relaxation dynamics in this case could be expressed by biexponential fits, with time constants  $\tau_1 \leq 0.1 \text{ ps}$  and  $\tau_2 \sim 1 \text{ ps}$  for all three ions. In earlier experimental work, Barbara et al. reported<sup>23</sup> the solvation dynamics around 7-dimethylaminocoumarin-4-acetic acid dissolved in water, giving biexponential time constants 0.16 and 1.2 ps. Subsequently, Jimenez et al.<sup>22</sup> studied the time dependence of solvation of coumarin 343 anion in aqueous solution. In this case, the relaxation dynamics were expressed by 0.12 and 0.88 ps.

#### IV. Conclusions

In this article, we have reported the relationship between the high degree of photoacidity of these molecules and electron transfer in excited states, by comparing fluorescence up-converted data of *N*-methyl-6- and 7-hydroxyquinolinium. The results presented here allow us to support the mechanism of tautomerization of 6- and 7-hydroxyquinoline in neutral water.

Excited-state proton transfer, electron transfer, and solvent relaxation processes in *N*-methyl-6-hydroxyquinolinium and *N*-methyl-7-hydroxyquinolinium were investigated in both acidic and basic media. The hydroxyl group behaves much like a superacid in the excited state: the deprotonation rates in *N*-methyl-6-hydroxyquinolinium and *N*-methyl-7-hydroxyquinolinium are  $(2 \text{ ps})^{-1}$  and  $(4.5 \text{ ps})^{-1}$ , respectively, and are among the fastest observed to date in intermolecular proton

transfer to water molecules. Such a very high photoacidity is explained by fast intramolecular electron transfer from hydroxylate ( $-\text{O}^-$ ) group to the positively charged pyridinium ring as soon as the proton transfer occurs. After proton ejection, which is the rate-limiting step in acidic solution, rapid intramolecular electron transfer occurs in  $<250 \text{ fs}$  to make  $\text{K}^*$  from  $\text{Z}^*$  form and followed by solvent relaxation in about 1 ps in both *N*-methyl-6-hydroxyquinolinium and *N*-methyl-7-hydroxyquinolinium. Experiments with even faster time resolution should provide a more quantitative assessment of the electron transfer rate between the two aromatic rings.

**Acknowledgment.** This work was supported in part by the American Chemical Society Petroleum Research Fund. We are grateful for the use of the Ti:sapphire laser, which was made available by Dr. Robin Hochstrasser through the Regional Laser and Biomedical Technology Laboratories at the University of Pennsylvania. T.G.K. acknowledges support by the National Institutes of Health.

#### References and Notes

- (1) Douhal, A.; Lahmani, F.; Zewail, A. H. *Chem. Phys.* **1996**, *207*, 477–498.
- (2) Douhal, A. *Science* **1997**, *276*, 221–222.
- (3) Bertran, J.; Oliva, A.; Rodriguez-Santiago, L.; Sodupe, M. *J. Am. Chem. Soc.* **1998**, *120*, 8159–8167.
- (4) Kelly, S. O.; Barton, J. K. *Science* **1999**, *283*, 375–381.
- (5) Lahmani, F.; Douhal, A.; Breheret, E.; Zehacker-Rentien, A. *Chem. Phys. Lett.* **1994**, *220*, 235–242.
- (6) Lee, S. I.; Jang, D. J. *J. Phys. Chem.* **1995**, *99*, 7537–7541.
- (7) Fang, W. H. *J. Phys. Chem. A* **1999**, *103*, 5567–5573.
- (8) Fang, W. H. *J. Am. Chem. Soc.* **1998**, *120*, 7568–7576.
- (9) Garcia-Ochoa, I.; Bisht, P. B.; Sanchez, F.; Martinez-Ataz, E.; Santos, L.; Tripathi, H. B.; Douhal, A. *J. Phys. Chem. A* **1998**, *102*, 8871–8880.
- (10) Bardez, E.; Devol, I.; Larrey, B.; Valeur, B. *J. Phys. Chem. B* **1997**, *101*, 7786–7793.
- (11) Kim, T. G.; Kim, Y. R.; Jang, D.-J. *J. Phys. Chem. A* **2001**, *105*, 4328–4332.
- (12) Harris, C. M.; Selinger, B. K. *J. Phys. Chem.* **1980**, *84*, 891–898.
- (13) Thistlethwaite, P. J.; Corkill, P. J. *Chem. Phys. Lett.* **1982**, *85*, 317–321.
- (14) Thistlethwaite, P. J. *Chem. Phys. Lett.* **1983**, *96*, 509–512.
- (15) Itoh, M.; Adachi, T.; Tokumura, K. *J. Am. Chem. Soc.* **1983**, *105*, 4829–4830.
- (16) Itoh, M.; Adachi, T.; Tokumura, K. *J. Am. Chem. Soc.* **1984**, *106*, 850–855.
- (17) Nakagawa, T.; Kohtani, S.; Itoh, M. *J. Am. Chem. Soc.* **1995**, *117*, 7, 7952–7957.
- (18) Bardez, E.; Chatelain, A.; Larrey, B.; Valeur, B. *J. Phys. Chem.* **1994**, *98*, 2357–2366.
- (19) Kim, T. G.; Lee, S.-I.; Jang, D.-J.; Kim, Y. J. *J. Phys. Chem.* **1995**, *99*, 12698–12700.
- (20) Bardez, E.; Fedorov, A.; Berberan-Santos, M. N.; Martinho, J. M. G. *J. Phys. Chem. A* **1999**, *103*, 4131–4136.
- (21) Mason, S. F.; Philp, J.; Smith, B. E. *J. Chem. Soc. A* **1968**, 3051–3056.
- (22) Jimenez, R.; Fleming, G. R.; Kumar, P. V.; Maroncelli, M. *Nature (London)* **1994**, *369*, 473.
- (23) Jarzeba, W.; Walker, G. C.; Johnson, A. E.; Kahlow, M. A.; Barbara, P. F. *J. Phys. Chem.* **1988**, *92*, 7039–7041.
- (24) Rips, I.; Klafter, J.; Jortner, J. *J. Chem. Phys.* **1988**, *88*, 3246–3252.
- (25) Rips, I.; Klafter, J.; Jortner, J. *J. Chem. Phys.* **1988**, *89*, 4299.
- (26) Ballard, R. E.; Edwards, J. W. *J. Chem. Soc.* **1964**, 4868–4874.
- (27) Schulman, S.; Fernando, Q. *Tetrahedron* **1968**, *24*, 1777–1783.
- (28) Bratzel, M. P.; Aaron, J. J.; Winefordner, J. D.; Schulman, S. G.; Gershon, H. *Anal. Chem.* **1972**, *44*, 1240–1245.
- (29) Maroncelli, M.; Fleming, G. R. *J. Chem. Phys.* **1987**, *86*, 6221–6239.
- (30) Engstrom, S.; Jonsson, B.; Impey, R. W. *J. Chem. Phys.* **1984**, *80*, 5481–5486.